

Water-Mediated Photochemical Treatments for Low-Temperature Passivation of Metal-Oxide Thin-Film Transistors

Jae Sang Heo¹, Jeong-Wan Jo¹, Jingu Kang¹, Chan-Yong Jeong¹, Hu Young Jeong², Sung Kyu Kim³, Kwanpyo Kim⁴, Hyuck-In Kwon¹, Jaekyun Kim⁵, Yong-Hoon Kim⁶, Myung-Gil Kim^{7}, and Sung Kyu Park^{1*}*

¹School of Electrical and Electronics Engineering, Chung-Ang University, Seoul 156-756, Korea

²UNIST Central Research Facilities, Ulsan National Institute of Science and Technology (UNIST), Ulsan 689-798, Korea

³Department of Materials Science and Engineering, Korea Advanced Institute of Science and Technology (KAIST), Daejeon 34141, Korea

⁴Department of Physics, Ulsan National Institute of Science and Technology (UNIST), Ulsan 689-798, Korea

⁵School of Advanced Materials Science and Engineering, Hanbat University, Daejeon 305-719, Korea

⁶School of Advanced Materials Science and Engineering, Sungkyunkwan University, Suwon, Korea

⁷Department of Chemistry, Chung-Ang University, Seoul, Korea

Corresponding authors

*E-mail: myunggil@cau.ac.kr (M.-G.K.) and skpark@cau.ac.kr (S.K.P)

Table of Contents

1. Table S1. Composition analysis of *a*-IGZO films with different annealing conditions.
2. Figure S1. Electrical characterization of DUV-irradiated AlO_x dielectric layer.
3. Table S2. The summarized electrical properties of DUV-irradiated AlO_x dielectric layer.
4. Figure S2. The transfer characteristics of DWD-annealed *a*-IGZO TFTs.
5. Figure S3. The statistical distribution of hysteresis voltages.
6. Figure S4. The threshold voltage shift of solution-processed *a*-IGZO TFTs under a negative gate-bias illumination stress (NBIS).
7. References.

1. Composition analysis of α -IGZO films with different annealing conditions.

The chemical composition analysis of for the diversely treated α -IGZO films (1h DUV, 2h DUV, DW, DWD) was performed with X-ray photoelectron spectroscopy (XPS) analysis and Energy Dispersive Spectroscopy (EDS). Within typical error range of EDS and XPS, the chemical compositions from XPS and EDS showed identical atomic ratios for the same samples, which are proportional to molar concentration of indium, gallium, and zinc precursors (In: 0.085 M, Ga: 0.0125 M, Zn: 0.0275 M).^{S1} The similar atomic ratios for entire α -IGZO samples confirm that the α -IGZO films maintained consistent chemical compositions during the diverse processing conditions, even after the water treatment.

Table S1.

Sample	Atomic %					
	In		Ga		Zn	
	XPS	EDS	XPS	EDS	XPS	EDS
1h DUV	69.53	69.43	6.87	7.51	23.61	23.06
2h DUV	68.79	73.61	7.25	6.58	23.96	19.8
DW	69.26	72.62	7.58	9.62	23.16	17.76
DWD	69.39	73.7	7.34	7.38	23.27	18.92

Table S1. Atomic composition ratio of 1h DUV, 2h DUV, DW, DWD-annealed α -IGZO films.

2. Electrical characterization of DUV-irradiated AlO_x dielectric layer.

The areal capacitance vs. frequency (C-F) and leakage current density vs. electric field (J-E) characteristics of the DUV-annealed AlO_x gate dielectric layer are shown in Figure S1. The areal capacitance of the DUV-annealed AlO_x gate dielectric layer was 120 nF cm⁻² at 100 Hz, showing a dielectric constant of 5.42. However, the capacitance value slight decreases with increasing frequency (104 nF cm⁻² at 1 MHz) which can be attributed to structural defects such as hydroxyl group or oxygen vacancies in the film.^{S2} Meanwhile, the DUV-annealed AlO_x gate dielectric showed an excellent insulating property as shown Figure S1(b). Particularly, the DUV-annealed AlO_x gate dielectric had a leakage current density of 7.14×10⁻⁸ A cm⁻² at 2 MV cm⁻¹ and a breakdown field of 7.8 MV cm⁻¹. Also, the distributions of leakage current density and dielectric breakdown field indicate that the DUV-annealed AlO_x gate dielectric has reasonable spatial uniformity over the tested substrate [Figure S1(c)].

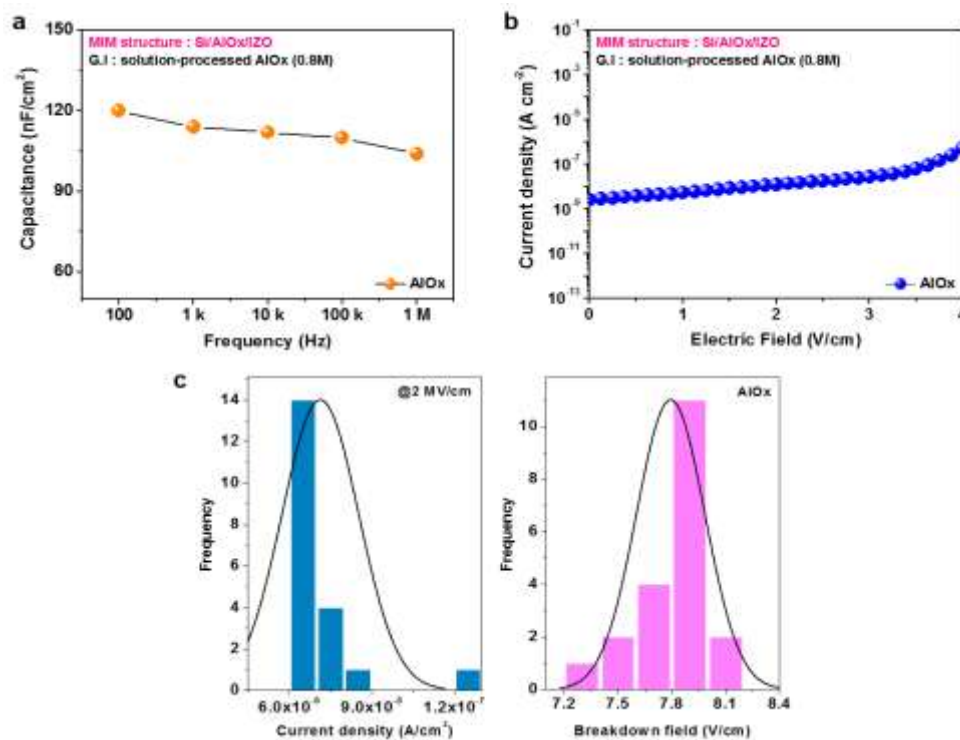


Figure S1. **a**, Capacitance per area-frequency (C-F) and **b**, Leakage current density-electric field (J-E) of AlO_x dielectric layer using M-I-M structure devices. **c**, Statistical distribution of current density and breakdown field of AlO_x dielectric layer.

3. The summarized electrical properties of DUV-irradiated AlO_x dielectric layer.

Table S2.

Sample	Breakdown field (MV/cm)	Current density (at 2MV/cm)	Capacitance (at 100 Hz)	Thickness	Dielectric Constant
AlO _x _DUV1h	7.8	$7.14 \times 10^{-8} \text{ A/cm}^2$	120 nF/cm ²	40 nm	5.42

Table S2. The electrical characteristics of DUV-irradiated AlO_x dielectric layer.

4. The transfer characteristics of DWD-annealed α -IGZO TFTs.

For experimental simplicity, we used simple glass container with water spray as sample water treatment chamber. Therefore, the relative humidity of 70-80% for water treatment is not the optimized condition in this study. To investigate the water content effect, we tested different water content, 50-55% RH and 100% RH at 24 ± 1 °C, which corresponds to absolute water content of ~ 12 and 22 g/m³. As shown in Figure S2, we do not observe any significant difference in device performance with water content increase. Compared with the water treated sample at 70-80% RH, the electrical properties of the water treated samples at both 50-55% RH and 100% RH show less than 10% difference.

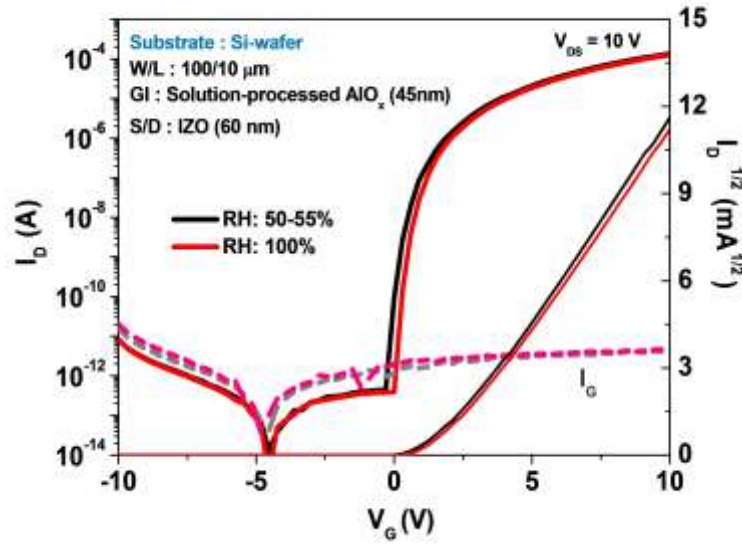


Figure S2. The transfer characteristics of DWD-annealed α -IGZO TFTs, which is stored at relative humidity of 50-55% and 100% for 1h.

5. The statistical distribution of hysteresis voltages.

We have defined the difference of threshold voltages (V_{TH}) obtained from forward gate sweep and reverse sweep current as hysteresis voltage.^{S3, S4} The hysteresis level of our device is consistently quite small for all devices. The representative transfer plot shows similar minimized hysteresis within device-to-device variation range. The average hysteresis voltages of 1h DUV-annealed, 2h DUV-annealed, DW-annealed, and DWD-annealed α -IGZO TFTs have 0.83, 0.73, 0.77, and 0.72 V, respectively.

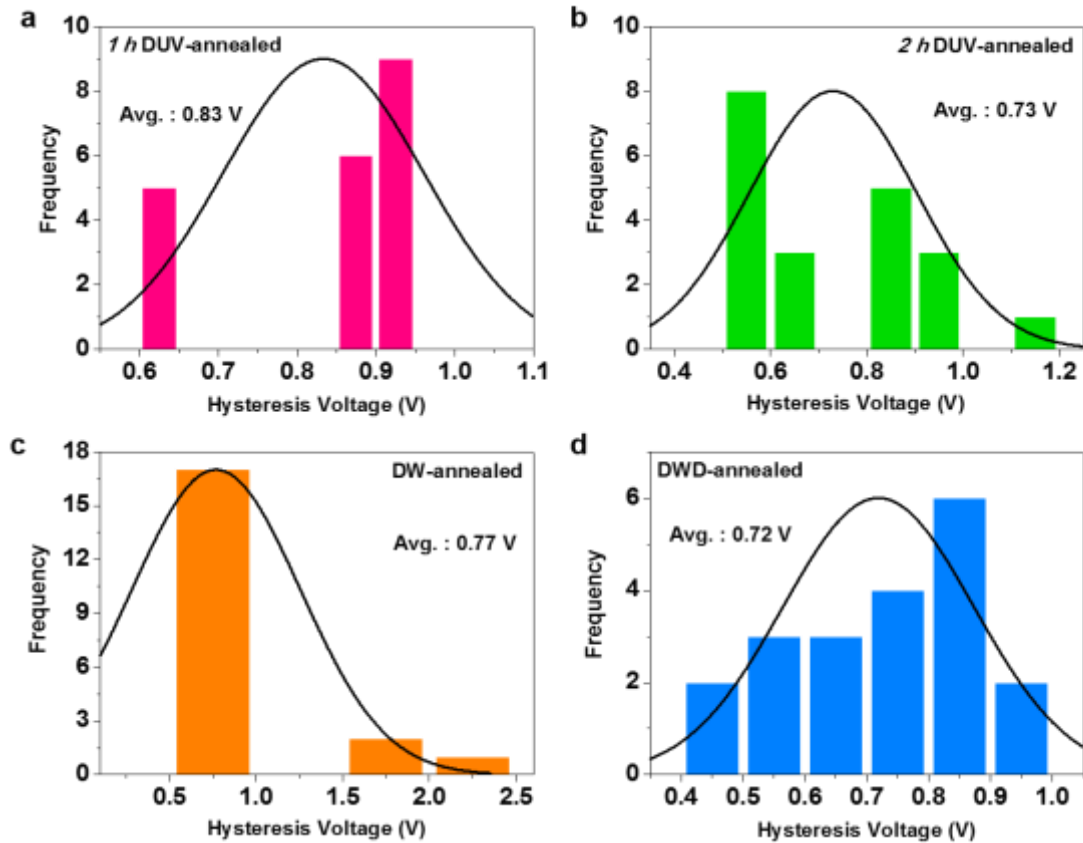


Figure S3. The statistical distribution of hysteresis voltages. **a.** 1 h DUV-annealed, **b.** 2 h DUV-annealed, **c.** DW-annealed, and **d.** DWD-annealed α -IGZO TFTs.

6. The threshold voltage shift of solution-processed *a*-IGZO TFTs under NBIS.

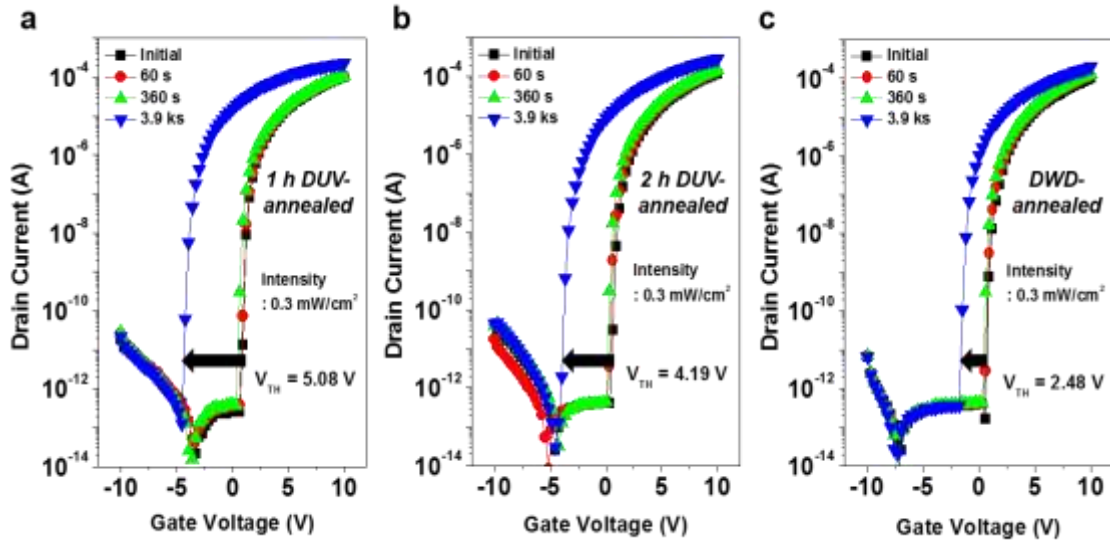


Figure S4. Threshold voltage shift of solution-processed *a*-IGZO TFTs under a negative illumination gate-bias stress (NBIS) ($V_{GS} = -5 \text{ V}$, $V_{DS} = +0.1 \text{ V}$, $t = 3,900 \text{ sec}$). (a) 1 h DUV-annealed, (b) 2h DUV-annealed, and (c) DWD-annealed *a*-IGZO TFTs.

7. References

- (S1) Waldo, R. A.; Militello, M. C.; Gaarenstroom, S. W. Quantitative Thin-Film Analysis with an Energy-Dispersive X-ray Detector. *Surf. Interface. Anal.* **1993**, 20.2: 111-114.
- (S2) Park, J. H.; Kim, K.; Yoo, Y. B.; Park, S. Y.; Lim, K.-H.; Lee, K. H.; Baik, H. K.; Kim, Y. S. Water Adsorption Effects of Nitrate Ion Coordinated Al₂O₃ Dielectric for High Performance Metal-Oxide Thin-Film Transistor. *J. Mater. Chem. C* **2013**, 1 (43), 7166–7174
- (S3) Qu, M.; Li, H.; Liu, R.; Zhang, S.-L.; Qiu, Z.-J. Interaction of Bipolaron with the H₂O/O₂ Redox Couple Causes Current Hysteresis in Organic Thin-Film Transistors. *Nat. Commun.* **2014**, 5, 3185.
- (S4) Yang, M. H.; Teo, K. B. K.; Gangloff, L.; Milne, W. I.; Hasko, D. G.; Robert, Y.; Legagneux, P. Advantages of Top-Gate, High-K Dielectric Carbon Nanotube Field-Effect Transistors. *Appl. Phys. Lett.* **2006**, 88 (11), 2004–2007.